ChemComm

Check for updates

Mesoporous alloy chiral nanoparticles with high production yield and strong optical activities†

Yicong Ma,[a] Lin Yang,[b] Yu Chen,[c] Xiaopeng Bai,[d] Geping Qu,[e] Tao Yao,[f] Xiangchen Hu,[c] Jianfang Wang, [iD][d] Zongxiang Xu,[e] Yi Yu [iD][c] and Zhifeng Huang [iD] *[f]

Applying galvanic replacement reactions (GRRs) to the host chiral nanoparticles (CNPs) is an exclusive method to generate alloy CNPs with mesoporous structures through chirality transfer. However, the GRR-mediated chirality transfer is too inefficient to impose strong optical activities on the alloy mesoporous CNPs (or m-CNPs). Here we dope the host with gold (Au) to significantly enhance the chirality transfer, and additionally employ the Au adhesion layer to increase the production yield (PY) of binary m-CNPs.

Chirality refers to an asymmetric configurational property in which an object cannot be superimposed on its mirror image. Chirality naturally occurs in biological systems that overwhelmingly exhibit homochirality, a unique property in which biological building blocks, such as amino acids and sugars, predominantly consist of one of two chiral configurations. Homochirality essentially results in a wide range of asymmetric biochemical processes and functions, and various physiological effects within biosystems are essentially associated with the stereochemical configuration and conformation of biomolecules. As a result, an enantioselective synthesis of molecules with controllable chirality, functioning as *e.g.* pharmaceutics and pesticides, has become one of the most important topics in modern chemistry.[1] Heterogeneous asymmetric catalysis, occurring at a liquid-chiral catalyst interface, has been developed for

[a] *Department of Physics, Hong Kong Baptist University, Kowloon Tong, Hong Kong SAR, China*

[b] *HKBU Institute for Research and Continuing Education Shenzhen, Guangdong 518057, China*

[c] *School of Physical Science and Technology, ShanghaiTech University, Shanghai, 201210, China*

[d] *Department of Physics, The Chinese University of Hong Kong, Shatin, NT, Hong Kong SAR, China*

[e] *Department of Chemistry, Southern University of Science and Technology, Shenzhen, Guangdong, 518055, China*

[f] *Department of Chemistry, The Chinese University of Hong Kong, Shatin, NT, Hong Kong SAR, China. E-mail: zfhuang@cuhk.edu.hk*

mass production of single-enantiomer molecules.[2] Currently, a new type of chiral catalyst, inorganic CNPs composed of structural chirality at the atomic/molecular scale,[3] has been introduced to control enantiopreference[4–7] *via* an enantiospecific interaction with molecular substrates.[8,9] Inorganic CNPs, fabricated *via* chirality transfer from either chiral ligands[10] or macroscopic rotation in the clockwise/counterclockwise direction,[11] generally have non-porous nanostructures.[12] Large surface-to-volume ratio of catalysts, resulting from *e.g.* structural porosification, is favoured for obtaining high PY. Therefore, generating inorganic m-CNPs is crucial for the asymmetric catalysis. GRR of silver (Ag) CNPs, serving as the host, was conducted in an aqueous electrolyte containing $HAuCl_4$, H_2PtCl_4 or H_2PdCl_4 to generate binary (Ag:Au, Ag:Pt and Ag:Pd, respectively) m-CNPs,[13] which is an exclusive approach to fabricate alloy m-CNPs, to the best of our knowledge. However, the m-CNPs generally have weak optical activity, which is generally characterized with circular dichroism (CD) referred to as the differential absorption (or extinction) of left-handed and right-handed circularly polarized light by a chiral object. Such low optical activity illustrates that the GRR-mediated chirality transmission is too insufficient[13,14] to provide high enantioselectivity in asymmetric syntheses.

Herein, we employ an Au adhesion layer on which the host Ag CNPs are deposited to significantly increase the PY of m-CNPs, and dope the host with Au to enhance the GRR-mediated chirality transfer and thus impose strong optical activities onto the binary m-CNPs.

Binary Ag:Au m-CNPs were fabricated through the GRR of the host Ag CNPs in an aqueous $HAuCl_4$ solution (Fig. 1a), according to[13]

$$3Ag(s,CNPs) - 3e^- \rightarrow 3Ag^+(aq) \quad (1)$$

$$AuCl_4^- + 3e^- \rightarrow Au(s) + 4Cl^-(aq) \quad (2)$$

The structural porosification has a thermodynamical origin of the balance in charge transfer whereby the precipitation of an Au atom on the host causes an oxidation (or dissolution) of three Ag atoms in the host.

Fig. 1 A gold (Au) adhesion layer (with a thickness (T_{AL}) of 20 nm) facilitates the formation of Ag:Au m-CNPs *via* GRR of the host Ag CNPs (with a nominal P of 8 nm and height (H) of 80 nm). Schematics: GRR (in a HAuCl$_4$ solution) of the Ag CNPs on a sapphire (a) without and (b) with the deposition of the Au adhesion layer, to form the binary Ag:Au m-CNPs. The host and m-CNPs have atomic-scale chirality composed of the chiral twisting of multiple achiral facets, represented with the "#"-like symbols. (c) The close-packed arrays of Ag CNPs, deposited on the Au adhesion layer, are (d) applied to the GRR for a duration (t_{GRR}) of 1 h, characterized with ultraviolet (UV)-visible-NIR spectroscopies of (I) extinction, (II) CD, and (III) anisotropic g-factor (c) and (d) LH: red and pink lines; RH: blue and cyan lines. Plots of (e) efficiency of chirality transfer R_g (eqn (4)) and (f) production yield (PY) of the binary m-CNPs (eqn (5)) *versus* T_{AL}, resulting from the 1 h GRR of the host. Insets: Scanning electron microscopy (SEM) top-down images of (c-I) the host and (d-I) Ag:Au m-CNPs; the grey regions in (c-III) and (d-III) represent A_h and A_m (eqn (4)), respectively; (f) SEM top-down image of the m-CNPs used to calculate N_m (eqn (5)).

A close-packed array of Ag CNPs, functioning as the host in the GRR, was deposited by glancing angle deposition (GLAD) on a supporting substrate of sapphire or silicon wafer (Fig. S1a-I and a-II, ESI†). The Ag CNPs, without a porous structure (inset in Fig. 1c-I), were sculpted in left-handedness (LH) and right-handedness (RH) *via* substrata rotation in the counterclockwise and clockwise direction, respectively.[15] The host, composed of a nominal helical pitch (P) of sub-10 nm owing to fast substrate rotation during GLAD (eqn (S1), ESI†), exhibits an extinction (resulting from localized surface plasmon resonance or LSPR) of the transverse and longitudinal mode at ≈ 370 nm and the visible-near infrared (NIR) region, respectively (Fig. 1c-I).[16] On resonance with the LSPR, the host exhibits bisignated CD peaks. Switching the helicity from LH to RH barely affected the LSPR but caused the CD spectrum to flip around the zero-CD axis (Fig. 1c-II), illustrating that the host has optical activity intrinsically ascribed to their helicity. The anisotropic g-factor, denoting a mean optical activity of individual CNPs in the array, is calculated by[17]

$$g = CD/16\,500Ext \qquad (3)$$

where CD represents the ellipticity (units: mdeg), and "Ext" is the extinction excited with linearly polarized light. The host Ag CNPs have the anisotropic g-factor of $\approx 10^{-3}$ (Fig. 1c-III).

The 1 h GRR of the host Ag CNPs caused the transverse LSPR and CD modes of the host to be significantly suppressed,

accompanied by the detection of the LSPR and CD signals at a wavelength of ≈ 580 nm assigned to the precipitated Au (Fig. 1d-I and d-II). Switching the helicity of the host from LH to RH also induced the CD spectrum of the GRR products to flip around the zero-CD axis. Furthermore, the GRR-treated CNPs appeared to have mesoporous structures (inset in Fig. 1d-I). These experimental results illustrate the formation of binary Ag:Au m-CNPs *via* the GRR-mediated chirality transfer from the host, with an efficiency evaluated by

$$R_g = A_m/A_h \qquad (4)$$

where A represents the integrated area of the anisotropic g-factor spectrum, and the subscripes "h" and "m" represent the host and m-CNPs (marked with the grey regions in Fig. 1c-III and d-III, respectively). An efficient chirality transmission has a large R_g value. The chirality transfer from the host Ag CNPs was evaluated to have a R_g value of ≈ 0.2 (Fig. 1e and Fig. S2-I, II, ESI†), indicating a poor chirality transfer. Moreover, the GRR-induced PY of the binary m-CNPs is calculated by

$$PY = N_m/N_h \qquad (5)$$

where N is the number of CNPs in a given area of the supporting substrate where the CNPs were deposited, characterized with scanning electron miscopy (SEM, *e.g.*, inset in Fig. 1f). The GRR of the Ag CNPs led to an average PY value of ≈ 0.5 (Fig. 1f), illustrating a loss of roughly half of the CNPs as a result of the

GRR. Such poor chirality transmission and low PY can be improved with the use of an Au adhesion layer on which the host CNPs were deposited (Fig. 1b). With tailoring the thickness of the Au adhesion layer (T_{AL}) in a range of 0–30 nm (Fig. S1 and S2, ESI†), the largest R_g value of 0.334 was achieved at T_{AL} = 20 nm (highlighted with pink background, Fig. 1e), $\approx$65% higher than that without the Au adhesion layer. The PY value significantly increased from $\approx$0.5 to $\approx$1.0 at $T_{AL} \geq$ 10 nm (Fig. 1f). Without the Au adhesion layer, the host Ag CNPs weakly attach to the smooth surfaces of the supporting substrate; hence, peeling off from the substrate during the GRR facilely occurs to result in the low PY of the m-CNPs. Therefore, the 20 nm-thick Au adhesion layer is adopted to enhance the GRR-associated PY of the alloy m-CNPs.

However, R_g = 0.334 illustrates that 66.6% of optical activity is sacrificed in the GRR-mediated chirality transfer, mainly owing to the structural porosification. We found that doping the host copper (Cu) CNPs with Au could facilitate the chirality transmission, because of the dopant Au functioning as a structural scaffold.[14] In this work, the doping was adopted to produce the Ag:Au m-CNPs with strong optical activities (Fig. 2a). Layer-by-layer GLAD was conducted to dope the host Ag CNPs with Au, leading to the formation of non-porous host $Ag_{(1-x)}Au_x$ CNPs where the atomic percentage x of the dopant Au was adjusted in a range of 0–0.25. Then, the 2 h GRR was applied to the binary host, which was attached to the 20 nm-thick Au adhesion layer (Fig. S3 and S4, ESI†). Monitoring the LSPR and optical activities of the host binary CNPs as a function of x and the GRR duration t_{GRR} (Fig. S5 and S6, ESI†) revealed that the GRR-mediated chirality transfer occurs the most efficiently at x = 0.15 for a given t_{GRR} (Fig. 2b). Without the doping of Au (*i.e.*, x = 0), R_g is 0.334 (for the RH-host) and 0.201 (LH) for t_{GRR} = 1.0 h, 0.183 (RH) and 0.273 (LH) for t_{GRR} =

1.5 h, and 0.090 (RH) and 0.113 (LH) for t_{GRR} = 2.0 h. For comparison, doping the host of Au with x = 0.15 significantly amplifies the R_g values: 0.844 (RH) and 0.997 (LH) for t_{GRR} = 1.0 h; 0.839 (RH) and 0.753 (LH) for t_{GRR} = 1.5 h; 0.277 (RH) and 0.271 (LH) for t_{GRR} = 2.0 h. Elongating the GRR generally tends to deteriorate the chirality transfer (Fig. 2b) and PY (Fig. S7, ESI†), because the GRR-induced structural porosification inevitably destroys the chiral structures. Furthermore, the rate of the GRR (r_{GRR}) was evaluated by characterizing the atomic percentage (at%) of Ag in the binary Ag:Au m-CNPs as a function of t_{GRR} (Fig. S8, ESI†). As shown with the evaluation (Fig. 2c), r_{GRR} slightly increases from 20.7 to 20.8% h^{-1} with an increase of x from 0.1 to 0.15, and then quickly decreases with an increase of x from 0.15 to 0.25 (having a decreasing slope of -11.6% h^{-1}). This illuminates that the 15% dopants Au serve as the structural scaffold to not only support the galvanic replacement but accelerate the structural porosification, which is advantageous for efficient chirality transfer to generate the binary m-CNPs with strong optical activities.
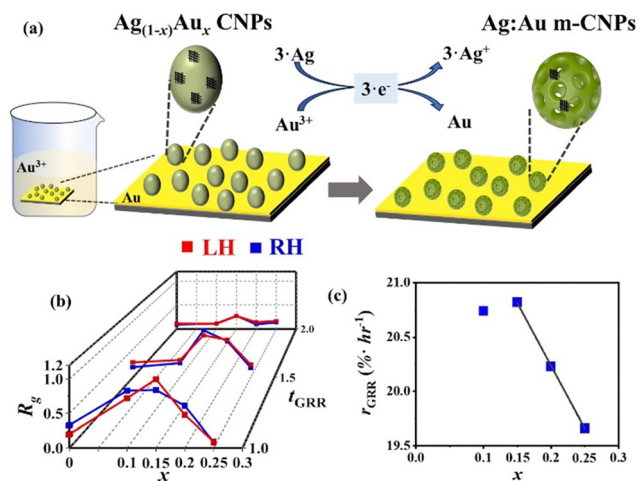

Fig. 2 Doping the host Ag CNPs with Au, which leads to the formation of the host $Ag_{(1-x)}Au_x$ CNPs, facilitates the GRR-mediated chirality transfer. (a) Schematic: GRR (in a $HAuCl_4$ solution) of $Ag_{(1-x)}Au_x$ CNPs attached to an Au adhesion layer (T_{AL} = 20 nm), to generate Ag:Au m-CNPs with strong optical activities. (b) Plot of R_g versus x and the GRR duration (t_{GRR}: 0–2 h). (c) Plot of the GRR reaction rate (r_{GRR}) versus x, which is linearly fitted (black line) at x of 0.15–0.25. (b) and (c) LH: red symbols; RH: blue symbols.
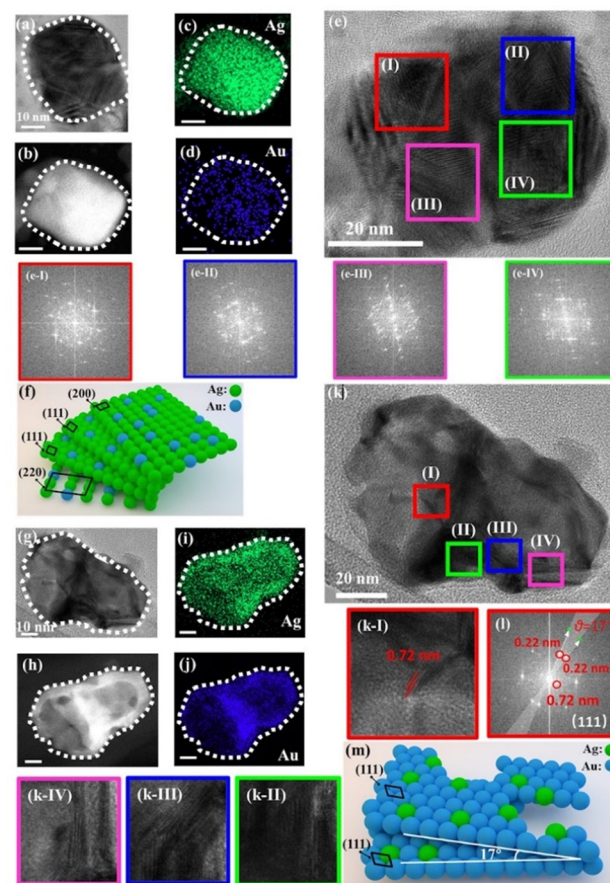

Fig. 3 Structural and elementary characterization of (a)–(f) the host RH-$Ag_{0.85}Au_{0.15}$ CNPs and (h)–(m) RH-Ag:Au m-CNPs (generated by the 1.5 h GRR of the host on the 20 nm-thick Au adhesion layer), using (a), (e), (g) and (k) transmission electron microscopy (TEM), (b) and (h) high-angle annular dark-field scanning transmission electron microscopy (HAADF-STEM), (c), (d), (i) and (j) mapping of energy dispersive spectroscopy (EDS), (e: I–IV and l) Fourier transform of the selected areas in (e) and (k-I), respectively. (f) and (m) Schematics of rotational Moiré patterns.

The 20 nm-thick Au adhesion layer and 15% dopants Au allow for optimizing the GRR-mediated chirality transmission and PY of the binary m-CNPs. To further understand the GRR-controlled chirality transfer, the host and the m-CNPs were comprehensively characterized. The host $Ag_{0.85}Au_{0.15}$ CNPs are composed of the solid-state solution without a mesoporous structure (Fig. 3a–e), and they are polycrystalline mainly consisting of the (111) facet (Fig. 4a). Many Moiré patterns were observed in the binary host (Fig. 3e), owing to chiral twisting of multiple achiral facets of (111), (200), and (220) (Fig. 3f). Such chiral twisting essentially imposes the chiroptical activity on the binary host.[18] More than two facets were involved in the chiral twisting, making the quantitative evaluation of the twisting angle difficult. The 1.5 h GRR porosifies the binary host (Fig. 3g), and the product Ag:Au m-CNPs are also made of the solid-state solution (Fig. 3h–j). Analogous to the binary host, the binary m-CNPs show many Moiré patterns (Fig. 3k). The GRR-induced porosification tends to preferentially destroy the minor (200) and (220) facets, resulting in the formation of the chiral twisting of two (111) facets in 17° (Fig. 3l and m). This characterization illuminates that the galvanic replacement of Ag with Au atoms in the chiral twisting lattices, particularly in the (111) facets, accounts for the GRR-mediated chirality transmission. The deterioration of optical activity with the elongation of GRR can be ascribed to the fact that the number of achiral facets involved in the chiral twisting reduces with the GRR-induced porosification. The galvanic replacement of Ag with Au can be verified by the suppression of the Ag 3d peaks (Fig. 4c) and amplification of the Au 4f peaks (Fig. 4d). The GRR-mediated alloying caused a downshift of the X-ray photoelectron spectroscopy (XPS) peaks compared to the binary host. The GRR also broadened the peaks

of the (111), (200) and (311) facets (Fig. 4b), ascribed to the porosification-induced decrease of the grain sizes.

In summary, GRR of the host Ag CNPs in $HAuCl_4$ enables the fabrication of binary Ag:Au m-CNPs. Doping the host with 15% Au atoms, which function as the structural scaffold to support the porosification and accelerate the galvanic replacement of Ag with Au, facilitates the chirality transfer from the host to the m-CNPs through replacing Ag with Au atoms in the chiral twisting (111) facets. The 20 nm-thick Au adhesion layer enhances the host-substrate adhesion, leading to a significant increase in the PY of the binary m-CNPs. This work devises an effective method to generate alloy m-CNPs with high production yield and strong optical activities. It provides an insight into understanding the GRR-mediated chirality transmission at the atomic scale, and paves the way to employing alloy m-CNPs for enantioselective synthesis of single-enantiomer pharmaceutics through heterogeneous asymmetric catalysis.

Conflicts of interest

There are no conflicts to declare.

References

1 A. Baiker, *Chem. Soc. Rev.*, 2015, **44**, 7449–7464.
2 I. Schrader, S. Neumann, A. Sulce, F. Schmidt, V. Azov and S. Kunz, *ACS Catal.*, 2017, **7**, 3979–3987.
3 L. Yang, J. J. Liu, P. Sun, Z. Y. Ni, Y. C. Ma and Z. F. Huang, *Small*, 2020, **16**, 2001473.
4 S. Li, J. Liu, N. S. Ramesar, H. Heinz, L. G. Xu, C. L. Xu and N. A. Kotov, *Nat. Commun.*, 2019, **10**, 4826.
5 X. Q. Wei, J. J. Liu, G. J. Xia, J. H. Deng, P. Sun, J. J. Chruma, W. H. Wu, C. Yang, Y. G. Wang and Z. F. Huang, *Nat. Chem.*, 2020, **12**, 551–559.
6 S. Butcha, S. Assavapanumat, S. Ittisanronnachai, V. Lapeyre, C. Wattanakit and A. Kuhn, *Nat. Commun.*, 2021, **12**, 1314.
7 Y. X. Fang, X. Liu, Z. P. Liu, L. Han, J. Ai, G. Zhao, O. Terasaki, C. H. Cui, J. Z. Yang, C. Y. Liu, Z. Y. Zhou, L. W. Chen and S. A. Che, *Chem*, 2023, **9**, 460–471.
8 P. Sun, J. J. Liu, M. Yan and Z. F. Huang, *Chem. Commun.*, 2018, **54**, 4270–4273.
9 L. Yang, J. J. Liu, J. H. Deng and Z. F. Huang, *InfoMat*, 2020, **2**, 1216–1224.
10 P. Kumar, T. Vo, M. J. Cha, A. Visheratina, J. Y. Kim, W. Q. Xu, J. Schwartz, A. Simon, D. Katz, V. P. Nicu, E. Marino, W. J. Choi, M. Veksler, S. Chen, C. Murray, R. Hovden, S. Glotzer and N. A. Kotov, *Nature*, 2023, **615**, 418–424.
11 W. F. Lau, L. Yang, F. Bai and Z. F. Huang, *Small*, 2016, **12**, 6698–6702.
12 L. Yang, P. Nandi, Y. C. Ma, J. J. Liu, U. Mirsaidov and Z. F. Huang, *Small*, 2020, **16**, 1906048.
13 J. J. Liu, Z. Y. Ni, P. Nandi, U. Mirsaidov and Z. F. Huang, *Nano Lett.*, 2019, **19**, 7427–7433.
14 Z. Y. Ni, Y. M. Zhu, J. J. Liu, L. Yang, P. Sun, M. Gu and Z. F. Huang, *Adv. Sci.*, 2020, **7**, 2001321.
15 Y. C. Ma, C. Lin, L. F. Cai, G. P. Qu, X. P. Bai, L. Yang and Z. F. Huang, *Small*, 2022, **18**, 2107657.
16 J. J. Liu, L. Yang and Z. F. Huang, *Small*, 2016, **12**, 5902–5909.
17 L. Yang, Y. Ma, C. Lin, G. Qu, X. Bai and Z. Huang, *Small*, 2022, **18**, 2200620.
18 Y. Ma, L. Yang, X. C. Hu, M. Zhang, G. P. Qu, X. P. Bai, H. F. Sun, F. Zhu, X. Y. Zhong, X. Chen, Z. X. Xu, Y. Yu and Z. F. Huang, *Adv. Opt. Mater.*, 2023, 2300696.
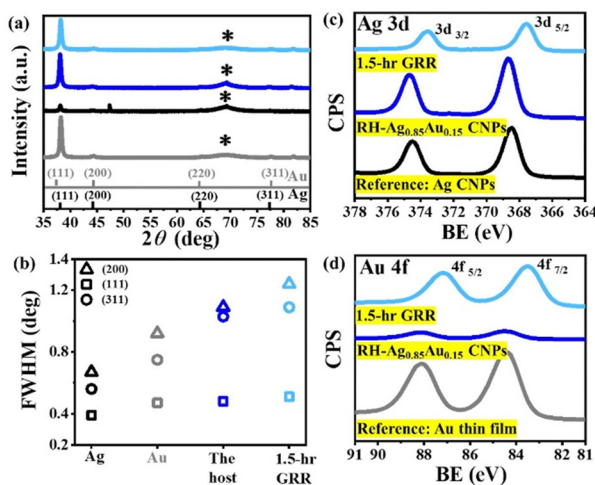

Fig. 4 Characterization of the host $RH-Ag_{0.85}Au_{0.15}$ CNPs and the RH-Ag:Au m-CNPs (produced by the 1.5 h-GRR of the host at T_{AL} = 20 nm) with (a) XRD and (c) and (d) XPS. (b) Plot of the full width of half maximum (FWHM) of the (111), (200) and (311) facets measured in (a). (a) The peaks marked with asterisks are assigned to the silicon wafers on which the CNPs are deposited. XPS: (c) Ag 3d; (d) Au 4f. Black and grey symbols: RH-Ag CNPs and Au thin films, respectively (as references); blue symbols: the host; cyan symbols: RH-Ag:Au m-CNPs.